Two- and Three-Dimensional Stacking of Chiral Alcohols

Coralie Alonso,[†] Franck Artzner,[‡] Bernadette Suchod,[†] Marcel Berthault,[§] Oleg Konovalov,[||] Jacques Pécaut,[⊥] Detlef Smilgies,[||] and Anne Renault*[,†,§]

Laboratoire de Spectrométrie Physique, UMR C5588, Université Joseph Fourier-CNRS, BP 87, 38402 Saint Martin d'Hères Cedex, France, Laboratoire de Physico-Chimie des Systèmes Polyphasés, UMR 8612, CNRS-Université Paris Sud, 5 rue J. B. Clément, 92296 Châtenay-Malabry Cedex, France, Groupe Matière Condensée et Matériaux, UMR 6626, Batiment 11A, Université de Rennes, 1, 35042 Rennes, France, ESRF, BP220, F-38043 Grenoble, Cedex, France, and CENG/DRFMC, avenue des martyrs, 38000 Grenoble, France

Received: December 23, 1999; In Final Form: January 16, 2001

An investigation of bulk single crystals and crystalline monolayers at the air−water interface of secondary alcohols bearing 16 and 17 carbons has been carried out in order to investigate their molecular packing. These "simple" chiral molecules can be seen as model systems; therefore, their study might provide broader knowledge of how chirality affects the molecular arrangement. The bulk racemic mixtures exhibit racemate organization, i.e., ordered mixtures of left and right enantiomers, with a head to head packing, whereas the pure enantiomers present a head to tail arrangement. The former type of motif has been reported for many amphiphilic molecules, whereas the latter is more rare. In two dimensions, all compounds, pure enantiomers, racemic mixtures, as well as other mixtures, present a hexagonal rotator phase with lattice parameters close to 5 Å. The rotational motion suggests the formation of a two-dimensional solid solution. However, upon heating, monolayers of 2-heptadecanol present a peculiar evolution. For mixtures of the two enantiomers with ratios between 1:1 and 2:1, the hexagonal phase transforms to a centered rectangular one, due to an inclination of molecules of about 10° with respect to the vertical. The loss of hexagonal symmetry is attributed to the formation of a racemate.

1. Introduction

The study of chiral molecules is of great interest in many different scientific fields ranging from nonlinear optics to pharmacology because of numerous potential industrial applications.[1−3] Enantiomeric molecules are chemically identical, but depending on their environment, chiral or not, they can have drastically different properties; thus, the importance of enantiomeric separation grows constantly with the development of pharmacology and drug design.[4] The focus is usually directed toward complex molecules of biological interest; however, for understanding fundamental concepts, aliphatic amphiphiles molecules present the advantage of being relatively "simple".[5,6] Moreover, they form highly crystalline phases in three (3D) as well as in two dimensions (2D) and can then be considered as interesting model systems for different purposes.[7] Their crystalline bulk and crystalline thin films have been well characterized, and in each case, the chains impose the overall packing.[8] However, it should be possible to at least induce a competition between the interactions involving the hydrocarbon chains as against those involving the chiral headgroup to determine the molecular arrangement. This should be the case in crystals of simple aliphatic molecules such as secondary alcohols bearing 16 (2-hexadecanol) and 17 (2-heptadecanol) carbons, for which the packing arrangement can only depends on hydrophobic and chiral interactions. These particular chain lengths were chosen because of previous investigations demonstrating that for shorter chain lengths, in 2D, the thermal motion is wide enough to yield rotator phases and thus hide the chiral interactions.[9,10] The aim of our study is to highlight the role of the chiral part of molecules on the 2D and 3D crystalline stacking of secondary alcohols and perhaps derive more general rules about packing of chiral molecules. In this paper, we describe the crystalline structures of bulk compounds and then those of monolayers spread at the air−water interface before drawing comparisons and infer some principles governing the two- and three-dimensional packing.

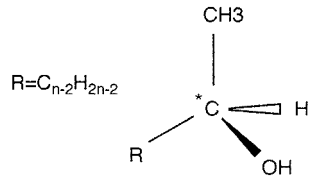

Figure 1. Schematic representation of a two-alcohol molecule. The * indicates the chiral center, the second carbon on the chain.

2. Experimental Techniques

Materials and Their Designations. The generic chemical formulas of a secondary alcohol is $C_nH_{2n+1}OH$. The chiral center is the second carbon, as shown in Figure 1. This study makes use of 2-hexadecanol ($n = 16$) and 2-heptadecanol ($n = 17$), racemic mixtures (±)2C*n* and left enantiomer (*S*)2C*n* for both. (±)2C16 was used as received from Fluka. (±)2C17, (*S*)2C16, and (*S*)2C17 were synthesized by copper-catalyzed Grignard methyl oxirane opening.[11] Other mixtures will be labeled (x_S-(*S*)/x_R(*R*))2C*n*, x_S being the ratio of *S* molecules and x_R the ratio

* To whom correspondence should be addressed. Fax: 33 2 23 23 67 17. E-mail: anne.renault@univ-rennes1.fr.
[†] Université Joseph Fourier-CNRS.
[‡] CNRS-Université Paris Sud.
[§] Groupe Matière Condensée et Matériaux.
[||] Université de Rennes.
[⊥] CENG/DRFMC.

10.1021/jp9944785 CCC: $20.00
Published on Web 11/29/2001

TABLE 1: Melting (T_m) and Crystallization (T_c) Temperatures of Bulks (3D) and Monolayers (2D) for Racemic Mixtures and Pure Enantiomers of 2-Hexadecanol and 2-Heptadecanol, (±)2C16, (*S*)2C16, (±)2C17, and (*S*)2C17, Respectively

	T_m, 3D (°C)	T_c, 3D (°C)	T_m, 2D (°C)	T_c, 2D (°C)
(±)2C16	43.0	29.0	41.5	44.5
(*S*)2C16	41.0	34.0	40.2	44.5
(±)2C17	36.0	34.0	49.0	50.8
(*S*)2C17	34.0	32.0	50.0	50.8

of *R* ones ($x_S = 100 - x_R$). The generic notation 2C*n* will be used when the ratio of both enantiomers is not a relevant parameter.

Bulk Study. Melting points of powder samples (quantities ≈ 1 mg) were determined by differential scanning calorimetry (DSC). A Perkin DSC II with sensitivity 20mcal/s was used with a scanning rate 10K/min in the temperature range (250−380 K). Melting temperatures reported in the following are those of the beginning of the melting.

Single crystals of 2C16 were obtained by slow evaporation of chloroform at a temperature of 6 °C. Single crystals of 2C17 were obtained by slow evaporation of xylene at room temperature. X-ray diffraction experiments were carried out at CEA-Grenoble on a Brucker three circles diffractometer. The diffracted beam was collected by a CCD two-dimensional detector. The wavelength was the Molybdenum radiation (0.710 73 Å). The sample was cooled to −80 °C by a nitrogen flow. Structures were solved and refined using the program Xtal3.2 (12). Heavy atoms were refined with anisotropic thermal coefficients, and hydrogen positions were calculated.

Monolayers Study. By depositing a drop of pure alcohol at the water surface, a monolayer spreads spontaneously and stays in equilibrium with the drop which plays the role of reservoir, able to compensate any loss of matter on the surface by evaporation or dissolution.[13] Temperature is then the variable thermodynamical parameter (see Table 1 to compare the melting points of monolayers and bulks). Laboratory techniques used to study monolayers at the air/water interface are ellipsometry and surface tension measurements. The setup has already been described in detail in ref 9. The crystalline structures have been characterized by grazing incidence X-ray diffraction (GIXD).[14] Experiments were carried out at ESRF (European Synchrotron Radiation Facility) in Grenoble, France. On a ID10B ondulator beamline, a double diamond monochromator selects a single radiation of $\lambda = 1.38$ Å. A double mirror deflects this beam onto the sample with an incident angle $\alpha = 2$ mrad $= 0.85\alpha c$ ($\alpha c = 2.3$ mrad critical angle for a water subphase at the energy of 9keV). The X-ray incident beam is monitored by a NaI scintillator. A Ge(111) crystal in position of Bragg reflection analyzes the diffracted beam, giving an angular resolution of $2.5° \times 10^{-3}$, corresponding to approximately 2.5×10^{-4} Å^{-1}. A position sensitive detector (PSD) collects the in-plane integrated intensity as well as the vertical distribution, thanks to its wide vertical aperture (15 cm). A special circular trough was designed for these experiments.[9]

3. Bulk Study

3.1. Thermodynamics. There are three ways of forming binary mixtures of enantiomers into organized arrays: racemate (ordered mixture), conglomerate (chiral separation), or solid solution (disordered mixture).[15] These three forms yield typical phase diagrams (melting temperature vs ratio of enantiomers), which can be established by DSC and thus allow the determination of the packing type. In Figure 2a, DSC spectra for powder samples of 2C16, measured upon heating, are depicted. One single exothermic peak is observed for concentrations of 50%, 90%, and 100% of (*S*) molecules, whereas two peaks are visible for other mixtures, the low-temperature one remaining invariant. The values are reported in the diagram in Figure 2b. An idealized representation of a typical diagram of a racemate is depicted in Scheme 1 for comparison. The existence of an eutectic point at lower temperature than that of the racemic mixture proves that 2C16 is a racemate. The result is the same for 2C17, as was already observed for shorter chains.[9]

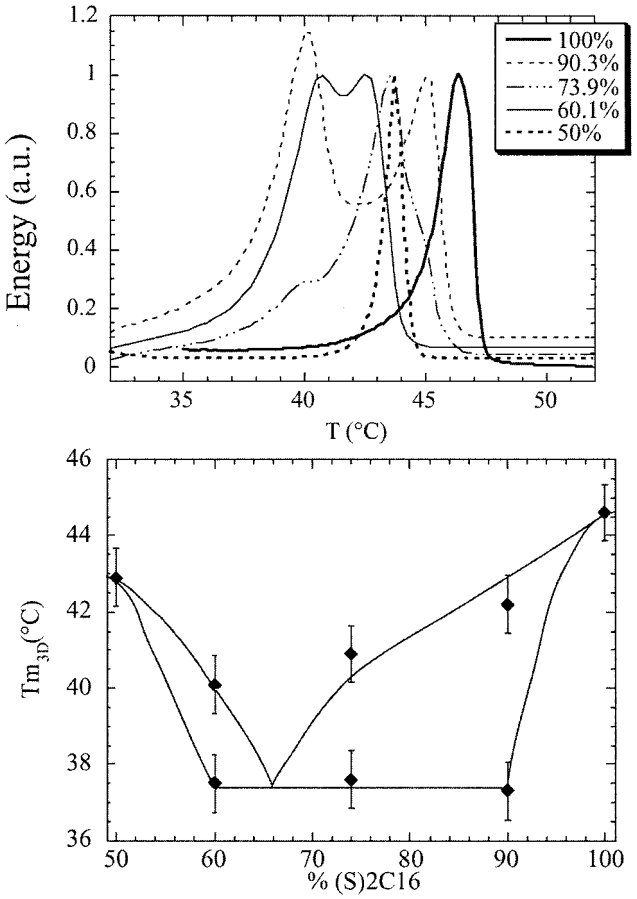

Figure 2. (a) DSC spectra of mixtures of 2-hexadecanol (2C16). The concentration of (*S*)2C16 within the sample is reported in the inset. (b) Phase diagram (melting temperature vs ratio of both enantiomers) of bulk 2C16. Lines do not correspond to any calculations.

SCHEME 1: Ideal Representation of the Diagram Melting Temperature as a Function of the Ratio of Both Enantiomers in the Sample, for a Binary Mixture of Enantiomers Forming a Racemate[a]

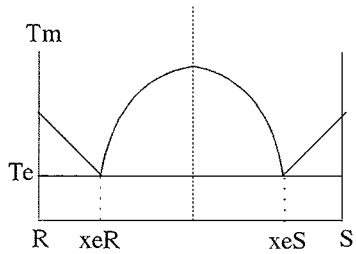

[a] T_E and x_E Are the Coordinates of the Eutectic Point. R and S Correspond to 100% of R and S Molecules.

3.2. Crystal Structures. *(±)2C16.* $C_{16}H_{33}OH$, Mw = 240 g/mol; triclinic, space group $P\bar{1}$; $a = 5.5818(2)$ Å, $b = 7.9076(3)$ Å, $c = 37.1269(9)$ Å; $\alpha = 93.449(1)°$, $\beta = 90.010(2)°$, $\gamma = 99.089(1)°$; $Z = 4$ (two crystallographically

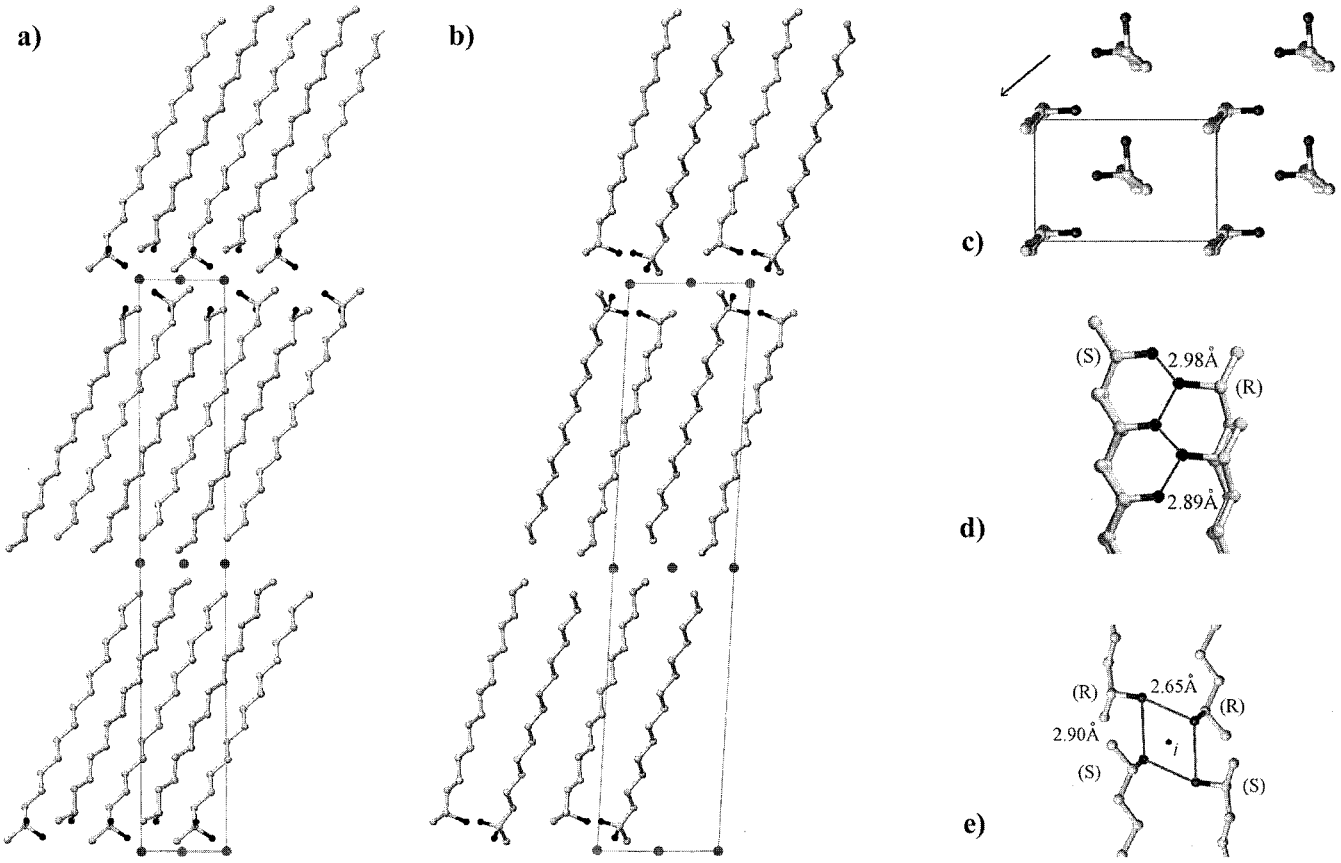

Figure 3. Crystalline structure of (±)2C16: $a = 5.5818(2)$ Å $b = 7.9076(3)$ Å $c = 37.1269(9)$ Å $\alpha = 93.449(1)°$ $\beta = 90.010(2)°$ $\gamma = 99.089(1)°$. One molecule in the unit cell presents enantiomeric disorder; the two equivalent positions for the O atom are reported. (a) View along the *b* axis. (b) View along the *a* axis: the circle indicates the inversion center. The structure can be described by a pseudo-orthorhombic subcell; $a_s = 4.94(2)$ Å, $b_s = 7.42(2)$ Å, $c_s = 2.54(1)$ Å, $\alpha = 91.5(5)$, $\beta = 90.5(5)$, $\gamma = 90.1(5)$. (c) View along c_s axis: the pseudo orthorhombic unit cell $O_\perp$ is represented. The arrows indicates the tilt direction. (d) View along the a_s axis and the hydrogen bonding for an heterochiral layer. (e) View along the a_s axis, showing the hydrogen bond tetramer of the homochiral structure.

independent molecules), $V = 1615.2(1)$ Å^3, $d_{calc} = 1.01(1)$g/cm^3; 5309 reflections, $R_w = 7.8\%$, $R = 10.2\%$ on refinement with 515 parameters.

Atomic coordinates and isotropic thermal factors are reported in the Supplementary Information, and the molecular arrangement is shown in Figure 3. The molecules are stacked in layers related by a center of symmetry, in a head-to-head organization usual for amphiphilic molecule structures.[8] The layer comprises the two independent molecules: the chirality of one is well defined (R for example), whereas the other exhibits enantiomeric disorder, i.e. has the same probability to be right- (*R*) or left-handed (*S*). If the two independent molecules within a layer are identical (RR or SS), each layer is homochiral, and the racemic crystal structure, labeled "homochiral", is an alternation of right-handed (*R*) and left-handed layers (*S*), related by a center of symmetry. If the two independent molecules within a layer are enantiomers (RS), each layer is heterochiral, and the racemic crystal structure, labeled "heterochiral", is an alternation of (*RS*) layer related by a center of symmetry. The disordered organization should be interpreted as the equiprobable superposition of the homochiral and heterochiral structures.

The carbon skeleton of the two independent molecules exhibits an all-trans conformation, including the methyl headgroup. The C−O bond is in a gauche position, roughly perpendicular to the main chain axis. The straight, regular hydrocarbon chains are arranged according to the common orthorhombic packing $O_\perp$, observed for *n*-tricosane or *n*-hexadecanol,[8,16] which implies a herringbone packing with a pseudoglide mirror (Figure 3c). Subcell parameters are $a_s = 4.94(2)$ Å, $b_s = 7.42(2)$ Å, $c_s = 2.54(1)$ Å, $\alpha = 91.5(5)$, $\beta = 90.5(5)$, and $\gamma = 90.1(5)$. The chains are tilted by 31.0(5)° from the layer normal in the $(a_s + b_s)$ direction, as indicated in Figure 3c. This tilt can be interpreted as a shift of two methylene groups along a_s and two methylene groups along b_s, as usually described for *n*-alcohols.[8,17] The average surface and volume per methylene group are 18.3 Å^2 and 23.2 Å^3, respectively.

The hydrogen bond network partially ensuring cohesion of the crystal is necessarily different for the heterochiral and homochiral structures. For the former, molecules are linked together by infinite chains of hydrogen bonds along the *a*-axis within a layer (Figure 3d). The shortest oxygen−oxygen distances are 2.89 and 2.98 Å. The lack of interlayer hydrogen bonds is the main characteristic of the heterochiral structure. In contrast, the homochiral structure develops interlayer hydrogen bonds through the formation of tetrameric oxygen cycles across the inversion center (Figure 3e) with oxygen−oxygen distances of 2.65 Å within the layer and 2.91 Å between layers. The condition for close packing of the methyl groups at the two ends of the molecules also plays a role in determining the layer stacking. At the head−head interface, the methyl in position 1 of a disordered molecule is surrounded by the CH chiral carbon, the oxygen of an ordered molecule, and the headgroup methyl of a disordered one, depending on the preferred conformation. The distances are, respectively, 3.85, 3.62, and 3.67 Å, corresponding to a close packed arrangement. At the tail−tail interface, the nearest-neighbor carbon−carbon distances are 3.94, 4.09, and 4.22 Å, which is in agreement with distances observed for *n*-alcohols.[16,17]

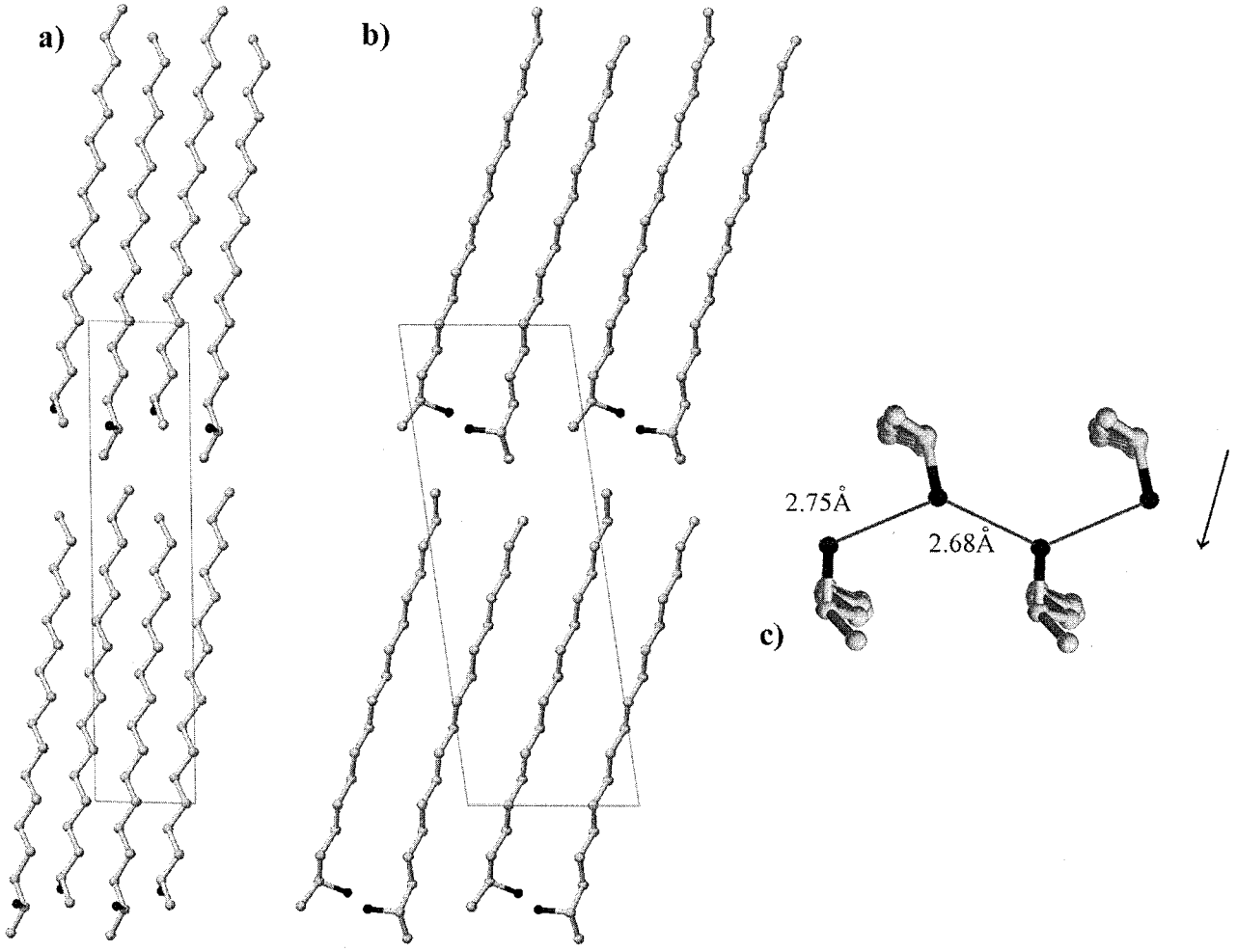

Figure 4. Crystalline structure of (*S*)2C17: $a = 4.85025(5)$ Å, $b = 8.1795(8)$ Å, $c = 22.912(2)$ Å, $\alpha = 81.915(8)°$, $\beta = 89.901(9)°$, $\gamma = 76.854(8)°$. (a) View along the *b* axis. (b) View along the *a* axis. The stucture can be described also by a triclinic subcell with $a_s = 4.1(1)$ Å, $b_s = 5.2(1)$ Å, $c_s = 2.54(2)$ Å, $\alpha = 73(1)°$, $\beta = 106(1)°$, $\gamma = 123(1)°$. (c) View along c_s, showing also the hydrogen bond network. The arrow indicates the tilt direction.

(S)2C17. $C_{17}H_{35}OH$, Mw = 254 g/mol; triclinic, space group *P*1; $a = 4.85025(5)$ Å, $b = 8.1795(8)$ Å, $c = 22.912(2)$ Å; $\alpha = 81.915(8)°$, $\beta = 89.901(9)°$, $\gamma = 76.854(8)°$; $Z = 2$ (two crystallographically independent molecules), $V = 873.5(15)$ Å^3, $d_{calc} = 0.97(2)$g/cm^3; 3735 reflections, $R_w = 8.0\%$, $R = 14.0\%$ on refinement with 317 parameters

Atomic coordinates and isotropic thermal factors are reported in the Supplementary Information, and the molecular arrangement is shown in Figure 4. The polar space group *P*1 is not frequently encoutered.[15] The molecules are stacked in layers, these layers related by translation resulting in a head-to-tail interlayer organization very uncommon for amphiphilic molecules[8] but previously observed.[18] Within the layer, the basic motif consists of two independent molecules related by a pseudo-2-fold axis (Figure 4c). Both molecules exhibit an all-trans conformation, including the methyl at the headgroup, so that the C−O bond is almost perpendicular to the main chain axis. The chains are tilted by 19(1)° in the direction perpendicular to the plane of the carbon backbone. The chains are all parallel to each other and arranged according to the triclinic packing motif T, observed for *n*-octadecane and the A-form of fatty acids.[8] The triclinic subcell parameters are $a_s = 4.1(1)$ Å, $b_s = 5.2(1)$ Å, $c_s = 2.54(2)$ Å, $\alpha = 73(1)°$, $\beta = 106(1)°$, and $\gamma = 123(1)°$.

The molecules are interlinked by hydrogen bonds of length 2.7(1) Å along the *a*-axis, namely, within the same layer, forming infinite chains (Figure 4c). Two oxygen atoms also make intralayer contacts with neighboring methyl groups with C−O distances of 3.67 and 3.96 Å, too long to allow the formation of hydrogen bond between these two atoms. The interlayer contacts are governed by methyl−methyl interactions with C−C distances of 3.79 and 3.95 Å.

Approximate Models of (±)2C17 and (S)2C16. Single crystals of (±)2C17 and (*S*)2C16 were also obtained, but their quality was not good enough to lead to properly refined structures.

The space group of (±)2C17 should be $P2_1/n$, with $a = 8.00(1)$ Å, $b = 4.96(1)$ Å, $c = 44.7(1)$ Å, $\beta = 91.51°$,[1] and a measured density of 0.96 g/cm^3. There are four molecules in the unit cell, related by symmetry. The length of the *c* axis is in agreement with a bilayer structure. The carbon atoms are in all-trans conformation; however, the position of the oxygen atom could not be determined, implying molecular disorder. The glide symmetry and the length of the $a = 8.00$ Å and $b = 4.96$ Å axes are compatible with an orthorhombic chain packing $O_\perp$ similar to that of (±)2C16. In the (±)2C17 structure, the molecules are tilted of about 15° along the *a* axis, as for the (*S*)2C17. Comparing the two racemic structures (±)2C16 and (±)2C17 recalls of the packing arrangement of alkanes[19] or *n*-alcohol;[20] namely, even numbered chains are tilted whereas the odd ones are not.[8] This odd/even effect is manifested in some physical properties, including the melting points.[21,22] We found a similar behavior for racemic secondary alcohols (Figure

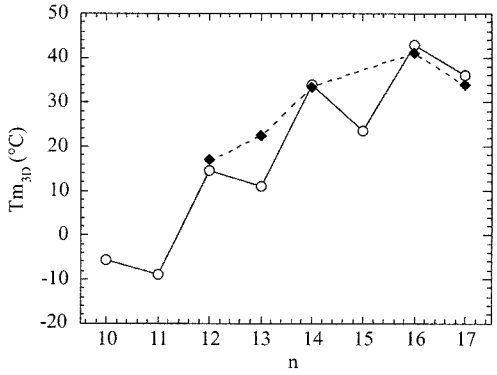

Figure 5. Comparison between 3D melting temperature of (♦) racemic mixtures and (O) pure enantiomers vs chain length *n* for secondary alcohols.

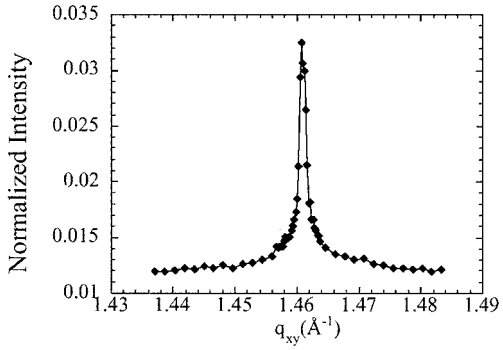

Figure 6. Diffraction pattern of a monolayer of (±)2C16 at $T = 41$ °C. The peak maximum is at $q_{xy} = 1.461$ Å^{-1}, and the full width at half-maximum corresponds to a coherence of a few micrometers.

5): melting temperatures are also strongly dependent on the parity of the chain, which can also be due to different packing energies due to different tilts.

For (*S*)C16, lattice parameters are $a = 4.81(1)$ Å, $b = 8.25(1)$ Å, $c = 42.63(1)$ Å, and $\gamma = 103.7°$,[3] and the density is 0.98 g/cm^3. α and β are 90° thus the space group should be monoclinic $P2_1$. Molecules are stacked in layers related by the 2-fold screw axis along *c*, resulting in a head to tail organization. The crystallographic motif within a layer consists of two molecules parallel to each other. All carbon atoms are in all-trans conformation, including the headgroup methyl; thus, chains are packed according to the triclinic packing T. This approximate model seems to be similar to that of (*S*)2C17, in terms of chain tilt also, which would be explain the monotonic evolution of melting temperatures with chain length for pure enantiomers (Figure 5).

3.3. Molecular Organization of 2-Alcohols. As for most chiral compounds, these particular secondary alcohols (2C16 and 2C17) crystallize as racemate. Wallach's rule states that racemate are denser than their chiral counterpart;[15,23] thus, for 2C16, this result could have been anticipated by comparing the densities of the (*S*)C16 (0.97 g/cm3) and (±)2C16 (1.01 g/cm^3). For 2C17, the pure enantiomer (*S*)2C17 and the racemic (±)-2C17 crystals have similar densities, ∼0.97 g/cm^3; thus, the Wallach rule is ambiguous. The origin of the heterochial behavior has to be found in the crystalline structure.

Orthorhombic chain packing $O_\perp$ is observed in racemic crystals of (±)2C16 and (±)2C17. The $O_\perp$ packing exhibits pseudoglide planes by construction.[25] Two independent molecules should be related by these pseudosymmetries, but then cannot be of the same handeness (*R* and *S*). Among the two hydrogen-bond axis possibilities along a_s or b_s, only along b_s are the oxygen−oxygen distances up to 3 Å, as exemplified by the (±)2C16 structure (Figure 3c). Because the pseudoglide mirror is perpendicular to hydrogen bond axis a_s the C−O bonds are shifted by $c_s/2$ (Figure 3d) and should originate in the tilt along a_s. Triclinic chain packing T is observed in the case of pure enantiomer crystals (*S*)2C16 and (*S*)2C17. The T packing exhibits a 2-fold axis by construction.[25] The carbon backbones of the two independent molecules are related by a pseudo-2-fold screw axis, which induces a shift of $c_s/2$ (Figure 4a). Consequently the 2-alcohol molecules must have the same handedness.

The all-trans chain conformation, independent of the chirality or the number of carbon atoms, indicates that the headgroup conformation is essentially imposed by the steric hindrance larger for the methyl group than the hydroxyl group, which is then in a gauche conformation. Nevertheless, secondary alcohols reproduce the same hydrogen bonds motifs as *n*-alcohols[24] but within a same layer due to the orientation of the hydroxyl group, almost perpendicular to the chain axis. The (*S*)2C17 and probably (*S*)2C16 structures accommodate a zigzag motif by shifting the molecules by one carbon atom (pseudo 2-fold screw axis) within a same layer. In the case of (±)2C16, the same hydrogen bond network can be formed for the heterochiral structure via the pseudoglide mirror. The similarity between 2C17 and 2C16 hydrogen-bonded lattices is clear by comparing the molecular packing along the *a* axis in Figure 3b and Figure 4b. The structure of (±)2C17 is not accurate enough to see a motif for the hydrogen bond network; however, the disorder can be seen as a way to have the same kind of hydrogen bonds on either sides of the layer.

4. Monolayers

The monolayers on water of pure enantiomers, racemic, and other mixtures of 2C16 and 2C17 have been characterized. These films are crystalline and stable with time at constant temperature.

4.1. 2C16 Monolayers, Enantiomeric, Racemic, and Mixtures. All these phases yield a single diffraction peak, indicative of a hexagonal arrangement of molecules (Figure 6). The lattice parameter $a_{hex} \approx 5$ Å is slightly longer than those of close packing of aliphatic chains; the thermal expansion rate is large (∼1.0 10^{-3} Å/K), and the Bragg peaks of the different phases are very narrow (coherence length is about 0.5 μm), typical of a rotator phase.[26] Whatever the ratio of (*R*) and (*S*) enantiomers, monolayers present the same hexagonal phase but with different lattice parameters. Our method of preparing monolayers allows the molecules to diffuse freely from the reservoir to the film and vice-versa; thus, the concentration in the monolayer is not necessarily the same as that of the reservoir drop.[27] Our results demonstrate that the interface does not favor one single ratio of enantiomers. This conclusion is confirmed by other experiments performed with a solid drop. In this case, the pressure is decreased by about 10mN/m, and we observed that (±)2C16 and (*S*)2C16 monolayers are no longer crystalline. However, for other enantiomeric mixtures, the condensed phase remains crystalline, still appearing in hexagonal symmetry but where the coherence length is affected, as exemplified in Figure 7, for the monolayer of (60(*S*)/40(*R*))2C16. The full width at half-maximum (fwhm) of the Bragg peak is larger when the drop is solid. The peak suddenly becomes narrower when the drop melts and the surface pressure rises. Such an evolution of the monolayer may be interpreted as a transition from a hexagonal to a rotator hexagonal phase at $T = T_m - 4$ °C. In Figure 7, one can also see a dramatic increase of the peak width one

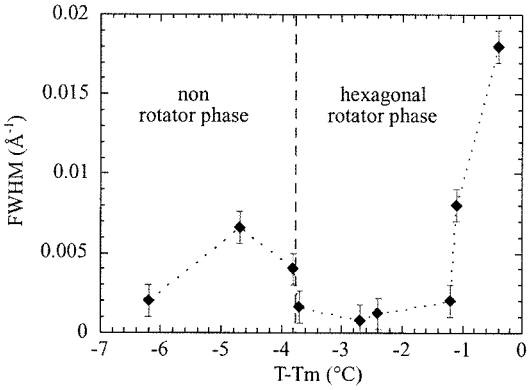

Figure 7. Evolution of full width at half-maximum (*fwhm*) for the Bragg peak of a (60(*S*)/40(*R*))2C16 monolayer vs (melting temperature T_m − sample temperature T).

TABLE 2: 2D Thermodynamical Phase Diagram of 2-Hexadecanol[a]

% (*S*)2C16	$T_m \pm 1$ (°C)	$a_L \pm 0.5$ (Å^2)	$\Delta S_m \pm 0.3$ (k_B)
50	43.6	29.1	7.3
60	43.2	27.4	5.7
75	42.8	28.1	6.7
90	–	–	–
100	41.2	28.8	7.1

[a] From left to right, the ratio of (*S*)2C16, melting temperature (T_m), area per molecule (a_L), and entropy (ΔS).

degree below the melting of the film. Surprisingly, it is only observed for the intermediate mixtures and not for pure compounds for which neither the intensity nor the width of peaks evolve with temperature. The decrease of crystallite size indicates that the monolayers of intermediate mixtures contain more defects than racemic or enantiomeric monolayers due to their "non ideal" enantiomeric ratios, which leads to a progressive softening of the film close to the melting. All these results are compatible with the observation that there is no spontaneous chiral separation of the molecules within the monolayers.

Additional information is necessary to distinguish between an ordered racemate or a solid solution. The "classic" phase diagram (melting temperature vs ratio of both enantiomers) has been established (see Table 2). The melting temperature was directly measured by ellipsometry, and the melting entropy was deduced from the slopes of surface tension versus temperature curves.[28] The melting temperatures and entropies for monolayers of (±)2C16 and (*S*)2C16 are almost the same. From these result, we may conclude that the racemic compound forms a solid solution since the formation of a racemate (ordered mixture) would imply a difference of at least the value of mixing entropy of the liquid phase, which is $Rln2 = 0.5k_B$, between racemic and enantiomeric phases.

4.2. 2C17 Monolayers, Enantiomeric, Racemic, and Mixtures. Monolayers of (*S*)2C17 have a behavior very similar to that of 2C16, namely, a hexagonal packing with a large coherence length (of about 0.5 μm) until the melting of the monolayer. However, for (±)2C17, the monolayer structure undergoes change upon heating. At low temperatures, a single diffraction peak is observed (Figure 8a), significant for a hexagonal phase. Increasing temperature induces a splitting of the Bragg peak (Figure 8b). These two peaks can be indexed as the {02} and {11} reflections of a centered rectangular cell $a = 5.01$ Å, $b = 7.50$ Å. The intensity distributions along the Bragg rods exhibit maxima at $q_z = 0.11$ Å^{-1}, corresponding to molecules tilted by about 10° from the surface normal along the direction of the *b* axis (Figure 8b), which explains the loss

TABLE 3: 2D Thermodynamical Phase Diagram of 2-Heptadecanol[a]

% (*S*)2C17	$T_m \pm 1$ (°C)	$a_L \pm 0.5$ (Å^2)	$\Delta S_m \pm 0.3$ (k_B)
50	49.1	30.0	8.6
60	49.5	28.9	7.3
75	49.0	30.2	8.4
90	49.5	29.5	7.7
100	50.0	29.6	7.8

[a] From left to right, the ratio of (*S*)2C17, melting temperature (T_m), area per molecule (a_L), and entropy (ΔS).

of hexagonal symmetry. This transition, from a hexagonal rotator phase to a herringbone arrangement, is reversible with temperature. A similar transition, but shifted from 43 to 44.5 °C, is observed for (75(*S*)/25(*R*))2C17. Similar solid−solid transitions have already been reported for long chain acids,[29] but this is the first time to our knowledge that a solid−solid transition in monolayers is found to be dependent on the ratio of enantiomers. Increasing the ratio of (*S*)2C17 in the sample shifts the transition temperature toward the melting temperature of the film. For a (90(*S*)/10(*R*))2C17 monolayer, this transition is no longer detectable since only one diffraction peak is observed, whatever the temperature. The hexagonal arrangement remains stable, however, close to the melting a softening of the monolayer is detected as for 2C16 mixtures. These results are summarized in Figure 9. This phase diagram contradicts the possibility of a chiral separation. Moreover the melting entropies of (±)2C17 and (*S*)C17 differ by $1k_B$; thus, this compound is probably a racemate (see Table 3).

5. Comparison between 2D and 3D Crystal Structures

The racemic mixtures of the 2-alcohols tend to pack in disordered heterochiral arrangement in both the two and three-dimensional crystals. In sections 3.3 and 4, we have shown that the chiral part of molecules plays an important role on the molecular arrangements. We can now compare the structures of a "free" monolayer at the water surface, and that of a layer within the three-dimensional counterpart.

The conformation of the carbon backbone was found to be all-trans in bulk crystals so that the C−OH bond is parallel to the layer plane participating in intralayer O−H···O hydrogen bonds. Regarding monolayers, the area per molecule, which is less than 21.5 Å^2, is consistent with an all-trans conformation. Previous studies of such monolayers on water had indicated that the C−OH bond points toward the water, which implies a gauche conformation of the methyl group at the water surface.[10] Thus, molecules at the air−water interface cannot be directly interlinked by O−H···O hydrogen bonds by rather make hydrogen bridges via water molecules from the subphase.

For the 2C16 alcohol, the 2D and 3D phases are similar both exhibiting disorder. In the racemate of the 3D system, the disorder is enantiomeric. The 2D structure exhibits rotational disorder, which masks any effect of chirality although the system has been identified as a solid solution. For the 2C17 alcohol, the racemic phases in 2D and 3D are similar, both being racemates. The (±)2C17 monolayer appears in a rectangular unit cell exhibiting a herringbone packing, implying a nonrotational phase, similar to the $O_\perp$ phase in the 3D crystal. The lattice parameters for the 2D and 3D counterparts are similar, slightly greater for the monolayer. In 2D crystals where molecules are freer to move in the horizontal plane, the competition between chain-chain and chiral interactions lead to larger distances between molecules. These effects should be enhanced by increasing the chain length, which would reduces

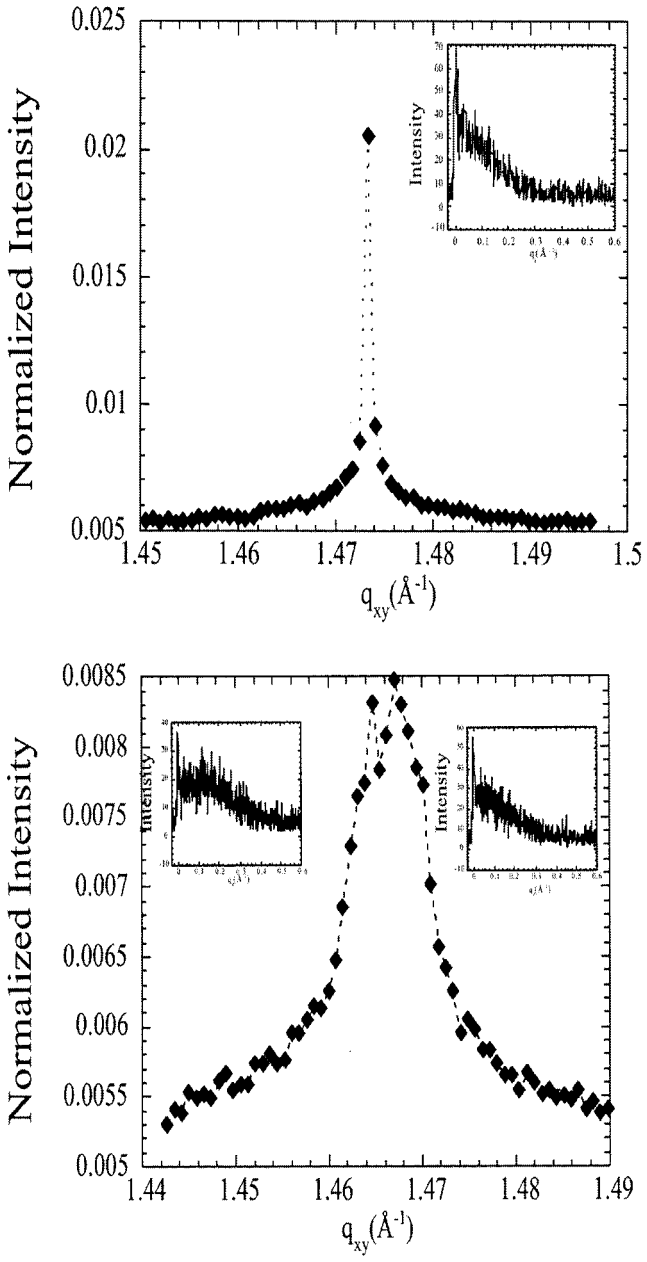

Figure 8. Diffraction pattern of a monolayer of (±)2C17. The insets are the intensity distributions along Bragg rod at the peak maxima. (a) $T = 43$ °C, $a_{hex} = 4.93$ Å, $fwhm = 3 \times 10^{-4}$Å^{-1}. (b) $T = 46.1$ °C, $a = 5.01$ Å, $b = 7.5$ Å, and the tilt angle is $\theta = 10°$.

the mean distance between chains because of van der Waals forces and thus enhance the influence of the chiral part on the molecular packing. This model is consistent with the observation that the racemic monolayer of the longest chain length studied (2C17) is not a solid solution.

Previous results show an odd/even effect on physical properties such as melting temperature for aliphatic compounds, alkanes or alcohols, in 3D crystals.[30] This effect is due to a difference in molecular tilt vis a vis the layer plane; the even chains are tilted, whereas the odd ones are not in order to optimize the packing of the terminal methyl groups. We observed an odd/even effect on melting temperatures for racemic bulks of 2-alcohols (Figure 5) which might be related to difference in tilt, as found in the structures of (±)2C16 and (±)2C17. An odd/even effect has also been previously observed in alcohol monolayers due to difference in orientation of their C−OH groups with respect to the water surface.[20] In contrast,

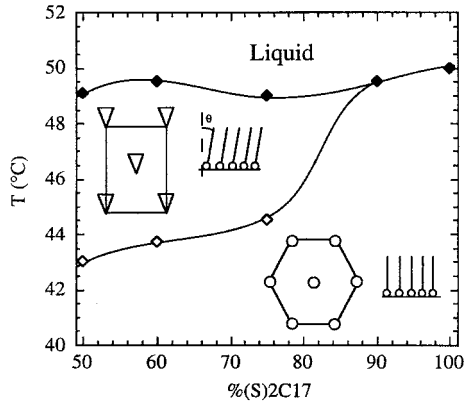

Figure 9. Schematic representation of the structural phase diagram of 2-heptadecanol (2C17) monolayers at the air−water interface.

the 2-alcohol molecules are aligned normal to the water surface for chain lengths between 12 and 16 implying no odd/even effect in two dimensions. The 2C17 is the only system we studied exhibiting tilted chains.

6. Conclusion

We have shown that (±)2C16 and (±)2C17 crystallize as racemate in three dimensions. In these structures, the molecules are stacked head to head into layers, within which cohesion is partially ensured by intralayer hydrogen bonding in addition to the obvious chain-chain interaction. The two compounds are disordered, identified as enantiomeric for (±)2C16. The layers in the pure enantiomeric crystals (*S*)2C16 and (*S*)2C17 are arranged head to tail, an unusual motif for amphiphilic molecules. The two-dimensional crystal structures of 2C16 and 2C17 on water are different: 2C16 forms a solid solution due to a high thermal disorder, whereas the 2C17 forms a racemate. This result seems to show that chiral interactions become more manifest for the longer chain system that we account for in terms of stronger chain−chain interactions with increasing chain length.

Acknowledgment. This paper is dedicated to Jean Jacques. We would like to acknowledge Bruno Berge for his great help during all this work as well as for experiments and many scientific discussions, Janine Lajzerowicz, and Michel Ollivon for many fruitful discussions, and Ivan Kuzmenko for the use of 2D fitting programs and many interesting discussions. Thanks also to Gérard Commandeur for his help during DSC experiments and Michel Bonin for X-ray diffraction data acquisition.

Supporting Information Available: Crystalline structure of (±)2C16 and (S)2C17: atomic coordinates and isotropic thermal factors for the two independent molecules in the unit cell. This material is available free of charge via the Internet at http://pubs.acs.org.

References and Notes

(1) Collins, A. N.; Sheldrake, G. N.; Crosby, J. *Chirality in Industry*; Wiley and Sons: Chichester, U.K., 1992; Vol. 1.

(2) Collins, A. N.; Sheldrake, G. N.; Crosby, J. *Chirality in Industry*; Willey and Sons: Chichester, U.K., 1997; Vol. 2.

(3) Batra, S.; Seth, M.; Bhaduri, A. P. *Prog. Drug Res.* **1993**, *41*, 191−248.

(4) De Bruin, T. J. M.; Marcelis, A. T. M.; Zuilhof, H.; Rodenburg, L. M.; Niederlander, H. A. G.; Koudijs, A.; Overdevest, P. E. M.; Van Der Padt, A.; Sudholter, E. J. R. *Chirality* **2000**, *12*, 627−636.

(5) Nassoy, P.; Goldmann, M.; Bouloussa, O.; Rondelez, F. *Phys. Rev. Lett.* **1995**, *75*, 457−460.

(6) Kuzmenko, I.; Weissbuch, I.; Gurovich, E.; Leiserowitz, L.; Lahav, M. *Chirality* **1998**, *10*, 415−424.
(7) Kuzmenko, I.; Rapaport, H.; Kjaer, K.; Als-Nielsen, J.; Weissbuch, I.; Lahav, M.; Leiserowitz, L. *Chem. Rev.* **2001**, *101* (6), 1659−1696.
(8) Small, D. M. *The Physical Chemistry of Lipids. Handbook of Lipid Research*; Plenum Press: New York, 1986; Vol. 4.
(9) Renault, A.; Alonso, C.; Artzner, F.; Berge, B.; Goldmann, M.; Zakri, C. *Euro. Phys. J., B* **1998**, *1*, 189−196.
(10) Alonso, C.; Blaudez, D.; Desbat, B.; Artzner, F.; Berge, B.; Renault, A. *Chem. Phys. Lett.* **1998**, *284*, 446−451.
(11) Kandil, A. A.; Slessor, K. N. *Can. J. Chem.* **1983**, *61*, 1, 1166.
(12) Hall, S. R.; Flack, H. D.; Stewart, J. M. *Xtal3.2 Reference Manual*; University of Western Australia, 1992.
(13) Renault, A.; Schultz, O.; Konovalov, O.; Berge, B. *Thin Solid Films* **1994**, *248*, 47−50.
(14) Als-Nielsen, J.; Jacquemain, D.; Kjaer, K.; Leveiller, F.; Lahav, M.; Leiserowitz, L. *Phys. Rep.* **1994**, *246*, 251−313.
(15) Jacques, J.; Collet, A.; Wilen, S. H. *Enantiomers, Racemates and Resolutions*; Wiley: New York, 1981.
(16) Abrahamsson, S.; Larsson, G.; Von Sydow, E. *Acta Crystallogr.* **1960**, *13*, 770−774.
(17) Precht, V. D. *Kiel. Milchwirtsch. Forschungsber.* **1974**, *26*, 221−254.
(18) Wang, J. L.; Leiserowitz, L.; Lahav, M. *J. Phys. Chem.* **1992**, *96*, 6, 15−16.
(19) Doucet, J.; Denicolo, I.; Craievich, A. F. *J. Chem. Phys.* **1981**, *75*, 1523−1529.
(20) Gavish, M.; Popovitz-Biro, R.; Lahav, M.; Leiserowitz, L. *Science* **1990**, *250*, 973−975.
(21) Broadhurst, M. G. *J. Res.* **1962**, *6A*, 241−249.
(22) Deutsch, M.; Wu, X. Z.; Sirota, E. B.; Sinha, S. K.; Ocko, B. M.; Magnussen, O. M. *Europhys. Lett.* **1995**, *30*, 283−288.
(23) Brock, C. P.; Schweizer, W. B.; Dunitz, J. D. *J. Am. Chem. Soc.* **1991**, *113*, 3, 9811−9820.
(24) Berstein, J.; Etter, M. C.; Leiserowitz, L. In *Structure Correlation* 2; Dunitz, H.-B. B., Ed.; VCH: Weinheim, 1994; pp 431−507.
(25) Kitaigorodskii, A. I. *Organic Chemical Crystallography*; Springer-Verlag: New York, 1984.
(26) Legrand, J. F.; Renault, A.; Konovalov, O.; Chevigny, E.; Als-Nielsen, J.; Grübel, G.; Berge, B. *Thin Solid Films* **1994**, *248*, 95−99.
(27) Alonso, C.; Artzner, F.; Lajzerowicz, J.; Grübel, G.; Boudet, N.; Rieutord, F.; Petit, J. M.; Renault, A. *Euro. Phys. J., E* **1999**, *3*, 63−70.
(28) Rieu, J. P., *Contribution a l'étude de la fusion cristallisation de monocouches d'alcools courts a la surface de l'eau.* Thesis, Université Joseph Fourier-Grenoble I, Saint Martin d'Hères Cedex, France,1995.
(29) Weidemann, G.; Brezesinski, G.; Vollhardt, D.; Möhwald, H. *Langmuir* **1998**, *14*, 6485−6492.
(30) Craievich, A. F.; Denicolo, I.; Doucet, J. *Phys. Rev. B* **1984**, *30*, 4782−4787.